

Received December 19, 2020, accepted December 29, 2020, date of publication January 4, 2021, date of current version January 13, 2021.

Digital Object Identifier 10.1109/ACCESS.2020.3049004

Design and Demonstration of a TDD-Based Central-Coordinated Resource-Reserved Multiple Access (CRMA) Scheme for Bidirectional VLC Networking

QIGUAN CHEN¹, DAHAI HAN¹, MIN ZHANG¹,
ZABIH GHASSEMLOOY², (Senior Member, IEEE),
ANTHONY C. BOUCOUVALAS³, (Fellow, IEEE), ZHIGUO ZHANG³,
TONGYAO LI¹, AND XIAOTIAN JIANG¹

¹State Key Laboratory of Information Photonics and Optical Communications, Beijing University of Posts and Telecommunications, Beijing 100876, China

²Optical Communications Research Group, Faculty of EE, Northumbria University, Newcastle upon Tyne NE1 8ST, U.K.

³Department of Telecommunications and Informatics, University of Peloponnese, 221 00 Tripoli, Greece

Corresponding author: Dahai Han (dahaihan@gmail.com)

This work was supported in part by the National Natural Science Foundation of China (NSFC) under Project 61975020 and Project 61705016, and in part by the Fundamental Research Funds for the Central Universities, China, under Project 2019RC12.

ABSTRACT The sharply growing demand for increased transmission capacity and bandwidth in last meter and last mile access networks together with the commercialization of fifth generation (5G) wireless systems has been opening up new opportunities for non-radio frequency (RF)-based wireless technologies. Visible light communications (VLC) technology is a potential candidate for access networking in 5G, which offers a higher spectral efficiency than RF-based Femtocell networks by three orders of magnitude. This paper proposes an all wireless optical bidirectional VLC multiple access scheme for pure VLC network access points in terminals. Centralized coordination is adopted to reduce the system complexity. And reservation of resource is introduced to guarantee collision avoidance during data frame transmission. The proposed multiple access scheme introduces special system parameters to achieve the balance of system throughput and access latency. The feasibility of the proposed scheme is verified by both theoretical analysis and experimental investigation. We show that the proposed scheme is suitable for a bidirectional pure VLC access network and can be used as a supplement in the IEEE 802.11 bb for 5G+bidirectional VLC application scenarios.

INDEX TERMS Bidirectional visible light communication networking, centralized coordination, multiple access, resource-reservation.

I. INTRODUCTION

With the gradual introduction of fifth generation (5G) wireless networks, the global mobile data traffic will continue to grow at a compound annual growth rate of 46 percent in 2022, reaching 77.5 exabytes per month [1], and thus poses challenging requirements for 5G networks [2], with new services, such as the Internet of things (IoT), big data and artificial intelligence (AI). As Fig. 1 demonstrates, visible light communications (VLC), which uses the license free

The associate editor coordinating the review of this manuscript and approving it for publication was Matti Hämäläinen¹.

visible band to offer higher data rates R_b , lower latency, low energy consumption and reduced implementation costs, is seen as a potential and complementary wireless technology in 5G and beyond networks [3], [4]. Therefore, the VLC-based network can help 5G networks meet the requirements of high-speed access and reliable services anywhere with real-time service and applications [5].

The license free VLC networking concept has attracted widespread attention. One of the most interesting investigations is the multiple access scheme that can push a VLC-based network to commercial use. Many studies have been carried out on this approach. Non-orthogonal multiple

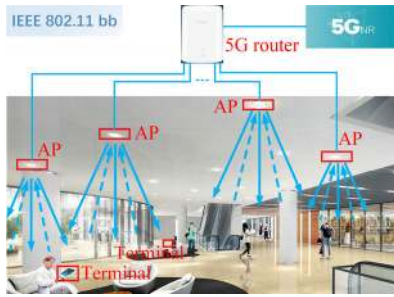


FIGURE 1. Application scenario of 5G+bidirectional VLC.

access (NOMA) has been recognized as a potential solution for VLC multiple users. NOMA mixed with a conventional OMA scheme was proposed in [6] for downlink visible light communication. In [7], NOMA was employed in downlink VLC for performance enhancement with a typical NOMA scenario with two users. A power line communications (PLC)-VLC network with a NOMA invoked in VLC to increase the downlink bit rate was reported in [8]. The researchers in [9] proposed a NOMA scheme for VLC based on single carrier transmission. In another study [10], the NOMA scheme was introduced to enhance the achievable throughput in high-rate VLC downlink networks. An optimization formulated as a multiobjective non-convex function using the cuckoo search (CS) algorithm was proposed for an NOMA-based VLC system for downlink transmission in [11]. Research on orthogonal frequency division multiplexing (OFDM) can enhance the utilization of the VLC frequency. In [12], orthogonal frequency division multiple access (OFDMA) was explored for VLC due to its high spectrum utilization efficiency and potentially high transmission data rate. A power line communication-VLC hybrid high data rate transmission approach with discrete wavelet transform (DWT)-based OFDM was designed and proposed for 5G communication systems in [13]. OFDM and multiple light-emitting diodes (LEDs) with spatial summing was developed to reduce the high peak-to-average power ratio (PAPR) in [14], OFDM-interleave division multiple access (IDMA) was applied in [15] to uplink a multiuser visible light communication system to solve inter-symbol interference (ISI) and multiple access interference (MAI) problems. A conventional code-division multiple access (CDMA) technique was also introduced to solve multiple user access for VLC. A multicarrier CDMA system based on an OFDM platform using an intensity modulation/direct detection scheme suitable for an indoor VLC environment was designed in [16]. CDMA combined with color-shift-keying (CSK) modulation was used in [17] for multiple access transmission for RGB-LED VLC to enhance the system capacity and mitigate light interference. An experimental demonstration of a VLC system employing CDMA resulting in a significant aggregate capacity improvement was reported in [18]. In addition, many other studies used multiple access and multiple access optimization for VLC systems, such

as a hybrid network with VLC for downlink transmission and radio frequency (RF) for uplink transmission [19], [20]. Moreover, an optimized solution for combined power and slot allocation in hybrid VLC/RF networks was proposed in [21]. M -ary pulse amplitude modulation was utilized to reduce channel inter-symbol interference (ISI) [22].

However, NOMA is a conventional power domain technique in which interference information is actively introduced at the transmitting end (Tx), while serial interference cancellation (SIC) technology with user signal power is correctly used at the receiving end (Rx). Thus, the receiver is considerably complicated and is not cost-effective for deployment and commercial applications. OFDM as a popular scheme suffers from nonlinear distortion due to a high PAPR. Furthermore, OFDM increases the signal interference (SI) due to subcarrier allocation to multiple users within the narrow bandwidth of commercial LEDs. Although CDMA is a representative of a conventional multiple access, the maximum number of users is limited due to the length of the spread code, ISI and MAI. In addition, in several previous studies, only downlink or uplink VLC communications was performed, and bidirectional VLC was even less considered.

As described in the light communication (LC) proposal in IEEE 802.11 bb Std. [23], two of the proposed use cases of VLC are combined with illumination and communications for an indoor scenario (office lighting and electromagnetic interference (EMI) sensitive areas with transmission distance < 10 m) and an outdoor scenario (streetlight-2-customer and vehicle-2-vehicle with transmission distance < 20 m). Both of indoor and outdoor use cases are the most commercially valuable, which can use a commercial LED as a light source for Tx and a photodiode (PD) for Rx. Thus, some qualification agreements must be followed to push VLC to large-scale applications:

(a) Due to the narrow modulation bandwidth of commercial white LEDs, FDM-based and CDMA-based schemes introduce interferences. Intensity modulation and direct detection (IM/DD) is the most feasible modulation for light communication. (b) Because of the characteristics of the direction and impenetrable nature of visible light, signal interference can be suppressed by the separation of Tx and Rx, and a narrow beam forms from Tx. Thus, a low implemental complexity of Rx and bidirectional transmission can be attained for the VLC system. In addition, (c), for large-scale deployment, cost-effectiveness should be taken into account.

Therefore, in practical cases, low complex time division duplex (TDD)-based multiple access is a prioritized choice. However, few pre-research efforts have been focused on TDD-based access for bidirectional VLC systems to date. Researchers in [24] addressed the bidirectional issue by proposing TDD for a single-user environment. The authors in [25] proposed a real-time LED-to-LED point-to-point bidirectional VLC system with a fast switcher between Tx and Rx to transmit and receive in the LEDs. An index time division multiple access (I-TDMA) was adopted to

provide spectral efficiency enhancement in [26]. In [27], a TDMA-like multiple access was considered with infrared for uplink transmission. Researchers in [28] proposed a carrier sensing multiple access with collision detection (CSMA/CD) mechanism for bidirectional vehicular visible light networks. A full-duplex request to send/clear-to-send (RTS/CTS) aided CSMA/collision avoidance (CA) mechanism was adopted to solve the hidden node problem in [29].

The previous efforts of TDD-based multiple access are motivating. However, pre-work on TDD-based multiple access scheme is only for a single-user environment regrettably [24]. In addition, the CSMA-based mechanism cannot thoroughly solve the problem of a hidden node because of the directional characteristic of visible light, which is an inherent obstacle for two nodes to hear each other.

In this paper, we propose a TDD-based central-coordinated resource-reserved multiple access (CRMA) scheme for a bidirectional multiple-user VLC system to solve the problems mentioned above with commercial white LEDs. Additionally, with the adoption of centralized coordination, as suggested in [30] and the IEEE 802.11bb Std., and the introduction of resource-reservation, the proposed scheme on the media access control (MAC) layer can be feasible for a bidirectional environment (which can be a supplement to the ongoing IEEE 802.11bb standard). Centralized coordination can solve the hidden terminal problem to render the bidirectional transmission feasible.

The contributions of this paper are as follows: (a) **Resources reservation:** The service cycle of the proposed multiple access scheme is sliced into two procedures: access procedure and data transmit procedure. In the access procedure, the terminals complete access and reserve resources (timeslots). Thus, the promised resource and collision avoidance during the data transmit procedure can be guaranteed. (b) **Low complexity:** Three handshakes occur during the access procedure, while no handshake occurs during the data transmit procedure, which reduces the complexity of the proposed scheme. (c) **Performance balance:** For TDD-based bidirectional transmission, three special parameters are suggestively introduced in the designed system to balance the system throughput and terminal access latency, which can meet application requirements of 5G/6G: extremely high throughput and ultra-low latency [31]. In addition, (d) **cost-effectiveness:** the designed system takes advantage of commercial and illumination-prioritized LEDs and PDs as Tx and Rx, which can cost-effectively support large-scale applications.

The remainder of the paper is organized as follows. In section II, we describe the system model and operation principle in detail. In section III, we carry out a performance analysis for the proposed scheme in terms of the system throughput and access latency. The experimental setup and results discussion are introduced in section IV, and an extended discussion follows in section V. Finally, conclusions are drawn in section VI.

II. SYSTEM DESIGN AND THE PROPOSED MULTIPLE ACCESS SCHEME

A. SYSTEM DESIGN

In the 5G+VLC application scenario shown in Fig. 1, the APs connect to a 5G router, providing bidirectional (both downlink and uplink) VLC links to a number of terminals. For the proposed typical indoor and outdoor user-cases of VLC networking [23], this paper designs TDD-based multiple access for bidirectional VLC networking, as demonstrated in Fig. 2. In the designed system, star topology is adopted, as shown in Fig. 2(a). Both the AP and terminal have an LED with a driver circuit as Tx and a PD with an amplifier and a filter as Rx. As shown in Fig. 2 (b), in a bidirectional VLC system, the key challenge is the interference at Rx. Fortunately, because of the inherent confinement of light, signal transmission has strong directivity. Both Tx and Rx have a cone to isolate Tx and Rx, and a lens to condense the light directivity. Therefore, the structure of a node (AP/terminal) can inhibit the self-interference originating from its own Tx directivity. Hence, the self-interference originating from a node's own Tx is mainly from the diffuse component of multiple path reflections, the scattering of photons projected onto solid molecules in the air near the node's own Tx and the reflection from the surface of an environmental objects (e.g., walls, floors, even the worn clothes of a human), which is very different from RF-based system. In [32] and in most practical cases, the influence of the diffuse component has no significant influence on the overall channel bandwidth, as it is masked by the strong LOS component. In addition, the researchers in [33] discussed in detail the interference for indoor VLC. Note that, Tx and Rx are physically different. Therefore, the designed system for bidirectional VLC networking is feasible. In addition, as shown in Fig. 2 (c), both the AP and terminal have the same MAC layer functional blocks with a difference block contention avoidance block for the terminal, which is discussed later. The key technique is the multiple access control, which is designed to schedule the terminal's uplink transmission.

B. BIDIRECTIONAL OPERATION

In the bidirectional system designed above, an AP with several terminals were designed. Both directions between the AP and terminals are optical links operated at the same frequency. As a fully centralized control scheme, the broadcast is designed for downlink transmission, while the TDD is designed for uplink transmission. In downlink transmission, the AP transmits frames continuously, where a control field contains the terminal's transmission control information to control the transmission timeslot of the terminals. Meanwhile, the terminals always receive the downlink frames. Thus, the transmission control information is obtained by all terminals. Therefore, the terminals can transmit frames by a comparison with the transmission control information (mainly the transmission timeslot). Note that, the transmission timeslot is authorized by AP during access procedure.

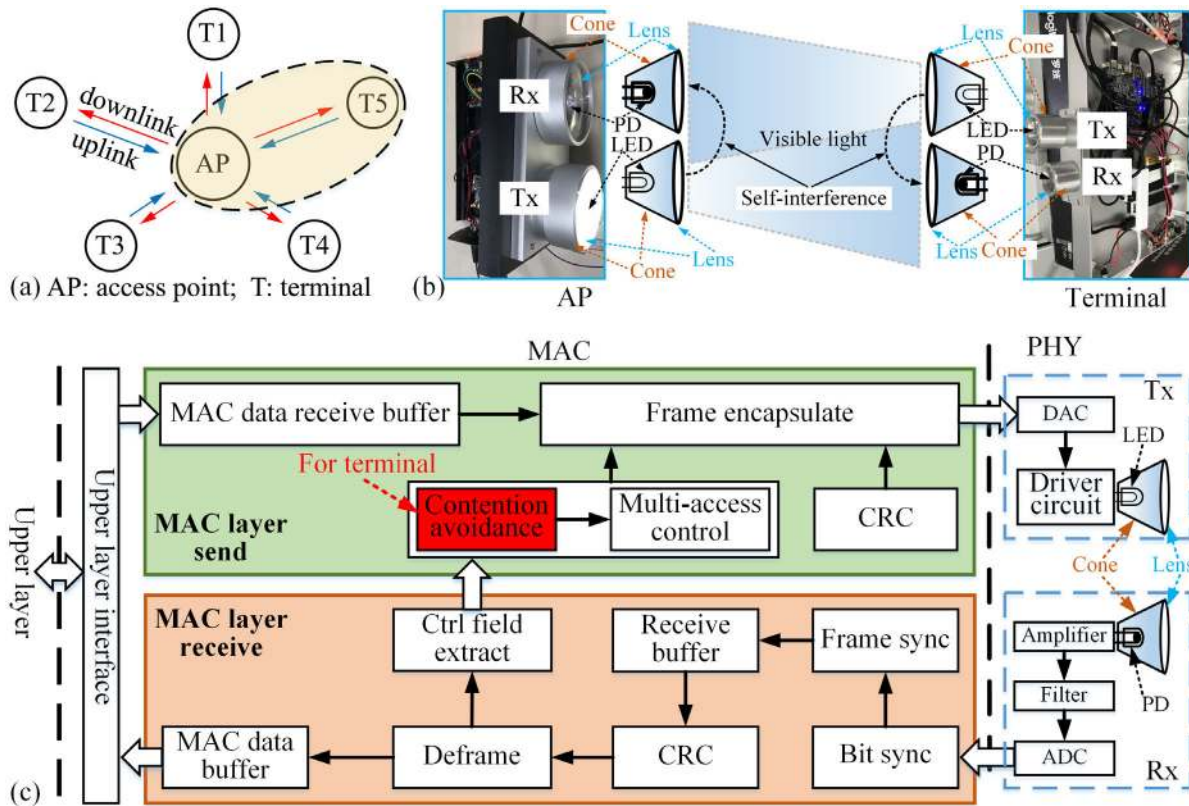


FIGURE 2. Topology and schematic diagram of CRMA for the bidirectional VLC networking system: (a) Bidirectional topology; (b) System model; (c) MAC layer functional blocks.

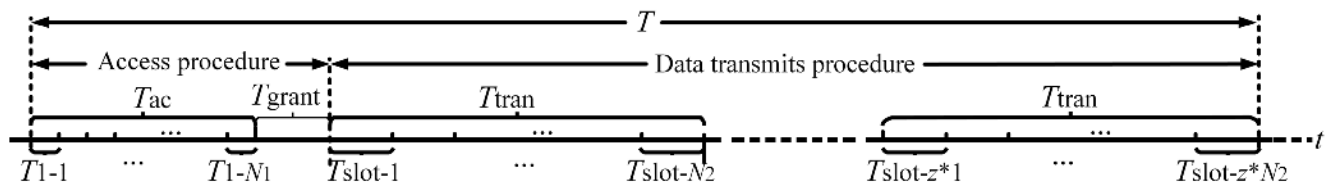


FIGURE 3. Schematic diagram of CRMA with special system parameters: N_1 , N_2 and z .

C. PRINCIPLE OF CRMA

The TDD-based CRMA proposed in this paper refers to the multiple access mechanism of an Ethernet passive optical network (EPON), and thus, for each terminal, multiple data transmissions are allowed. CRMA is controlled by the AP [30], supports pure VLC networking including both downlink and uplink channels, and introduces special system parameters, namely, N_1 , N_2 and z , for an improvement in bandwidth utilization and an enhancement of the system throughput without too much access delay. Hence, the capacity of the designed system can change easily according to system performance with a variation in the parameters N_1 , N_2 and z .

The TDD-based CRMA scheme slices the operation time into service cycles, and each service cycle T is composed of a single terminal access procedure and a data transmission

procedure. As depicted in Fig. 3, the access procedure is divided into T_{ac} (namely, the terminal access window) = $N_1 T_1$ ($N_1 = 1, 2, 3, \dots$) and T_{grant} (for AP grants). The data transmits procedure $T_{dtp} = z T_{tran}$, where $z = 1, 2, 3, \dots$, and $T_{tran} = N_2 T_{slot}$, where $N_2 = 1, 2, 3, \dots$, T_{tran} maintains the same grant sequence (T_{slot} sequence) according to T_{grant} . In the data transmit frames, timeslot arbitration is controlled by the AP, where transmission is broadcasted in each timeslot to the terminals, as shown in Fig. 3. At the terminals, the verifications of timeslot arbitration from the AP are carried out prior to uplink transmission at the assigned timeslot with collisions at the AP Rx. Note that T_{dtp} is contention free.

One of the characteristics of the proposed scheme is that both downlink and uplink transmission are based on the slot (T_1 in T_{ac} and T_{slot} in T_{dtp}). The downlink transmission uses the broadcast channel, and broadcast data in every T_{slot} ,

whereas the uplink channel is waiting for the slot of terminals (for access request: T_1 in T_{ac} , and for data transmits: T_{slot} granted by AP). This characteristic can improve the bandwidth utilization and save the cost of system synchronization.

1) TERMINAL ACCESS, TERMINAL CONTENTION AVOIDANCE AND RESOURCES RESERVATION MECHANISM

During the terminal access procedure, which has three phases, terminal access, terminal contention avoidance and resources reservation mechanism are carried out simultaneously. (i) The AP broadcasts, with size information and the start time of the access window, to all terminals simultaneously for permission to allow the unaccessed terminals to access the AP within T_{ac} . Note that all unaccessed terminals receive the access frame request prior to the connection to the AP. (ii) The terminal requesting the access generates a random back-off delay τ_{bd} followed by requests to access to the AP. Notably, for the proposed multi-access scheme, generally $\tau_{bd} = xT_1$, where x is a random natural number between 0 and N_1 , and T_1 is the access timeslot. For example, for the l_{th} and $(l+1)_{th}$ terminals, the delays are xT_1 and yT_1 , respectively. Notably, for the most cases $x \neq y$, and otherwise, the AP receives two optical signals simultaneously, thus resulting in a collision at the AP Rx and an error grant occurrence. Note that the terminals with a collision will not identify the error grants and need to re-request access in the next T_{ac} . The collision can be mitigated if $\tau_{bd} = NT_1$, where $N = 1, 2, 3, \dots$, with an appropriate probability distribution, such as a binomial probability distribution, and Poisson distribution. Notably, when a terminal requests access, it simultaneously requests a resources reservation according to the terminal's own demand. (iii) Finally, during T_{grant} and with a single grant frame at a time, the AP allocates all connected terminals with a timeslot (resource) to allow data transmission at T_{dtp} . Note, the number of data transmit frames depends on the number of access and connected terminals. The schematic flowchart of access procedure is shown in Fig. 4.

2) SYSTEM SYNCHRONIZATION

In the downlink broadcast channel, all terminals in AP coverage will receive the signal and synchronize with the AP with a synchronization module (i.e., a bit synchronize circuit) through a preamble sequence. Then, the terminal starts to detect the frame header, and begins to receive the downlink frame. Through the control field, the terminals determine the statues (access procedure or data transmits procedure) and make the uplink reaction (request to access, or transmit data, or no reaction). In the proposed multiple access scheme, T_{ac} and T_{grant} occur in every T cycle. Each access control in T_{ac} (granted in T_{grant} or data in T_{slot}) is broadcasted to all the terminals, which ensures that the system synchronization scheme performs well. Once a terminal synchronizes to the AP, it synchronizes with all the other terminals. Thus, each terminal knows when to transmit access request or data.

Notably, the synchronization of terminals is independent of each other.

3) CENTRALIZED ARBITRATION SLOT MANAGEMENT

The method of centralized arbitration slot management (CASM) is proposed for the AP (modify N_2) to manage the terminals' connectivity dynamically. When a new terminal has access to the AP in T_{ac} , the AP increases the number N_M of the active terminals. If a terminal leaves the AP, then it will delete the inactive connection and renew N_M . If there is no data in T_{dtp} and no request in T_{ac} , then the AP will make the terminal inactive and renew N_M before the terminal's re-access in the next T_{ac} to save the capacity resources.

D. COMPLEXITY COMPARISON

As discussed above, the proposed CRMA scheme reduces the complexity of the implementation. A comparison of the proposed CRMA scheme with the two main TDD-based multiple access schemes, namely, CSMA-based and RTS/CTS, is listed in Table 1. From Table 1, with one more handshake during the access procedure, during the data transmit procedure, the handshake, carrier sensing and random back-off before data transmission and collision are unnecessary in the proposed CRMA, which means that the implemental complexity can be reduced.

TABLE 1. Comparison of CRMA with a Conventional Multiple Access Scheme Used in Wireless Networking.

Multiple access scheme	Access procedure	Data transmits procedure			
		Handshake before data transmission?	Carrier sensing before data transmission?	Random back-off before data transmission?	Collision during data transmission?
CSMA-based	2	Yes	Yes	Yes	Yes
RTS/CTS-based	2	Yes	Yes	Yes	Yes
CRMA	3	No	No	No	No

III. SYSTEM METRICS

The MAC layer proposal simulation methodology for IEEE 802.11bb includes the system level with throughput and access latency [34], [35]. In this part, the system metrics of the proposed scheme in terms of the throughput and access latency is discussed and investigated based on a continuous T_{tran} with the special system parameters adopted above. The service cycle $T = T_{ac} + T_{grant} + \sum_{i=1}^{K-1} iT_{slot}$, where $K = 1, 2, 3, \dots$, etc. We assume that (i) the maximum user's capacity is $M = N_2$, where $N_2 = T_{tran}/T_{slot}$ is the number of timeslots; (ii) $T_{ac} = N_1T_1 + T_{grant}$, where $N_1 = 1, 2, 3, \dots$, etc., and T_{ac} is the access procedure; (iii) there are no error grants in

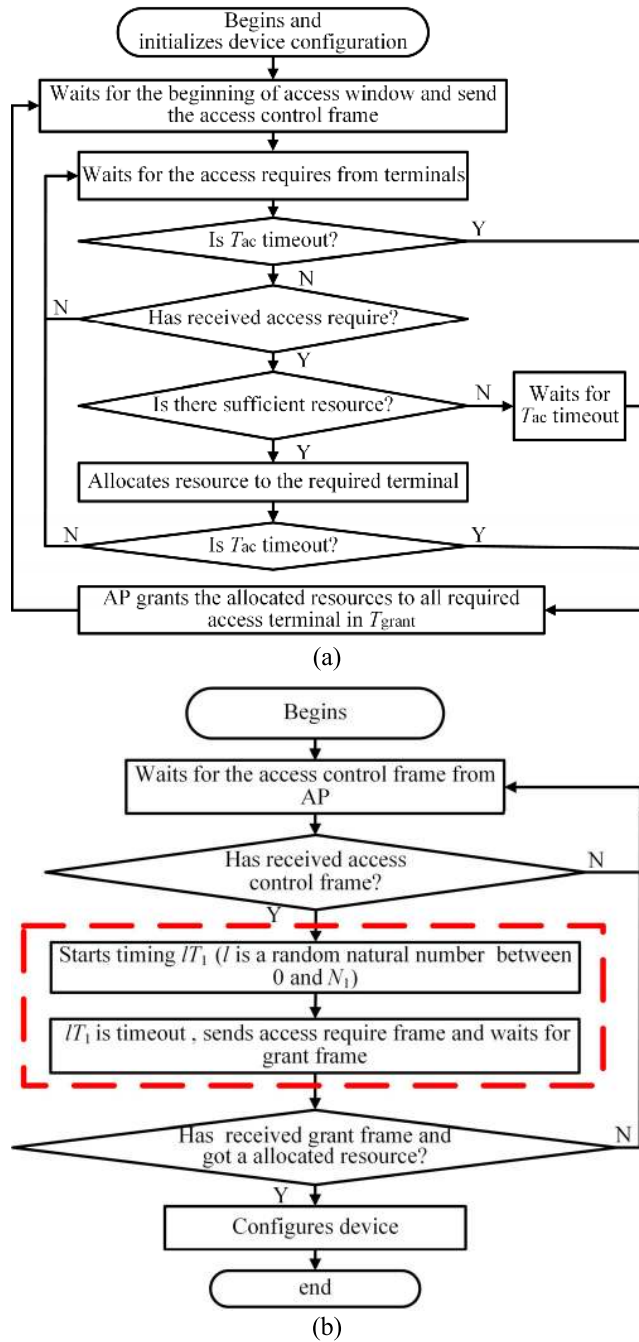


FIGURE 4. Schematic flowchart of the access procedure: (a) AP centralized control multiple access; (b) terminal access control with contention avoidance (red dashed line).

T_{grant} ; (iv) the same priority is applied to all transmissions; and (v) each terminal and the AP in the network always have packets to transmit.

A. SYSTEM NORMALIZED THROUGHPUT

The normalized link throughput is defined as the ratio of the time the channel used for the successful transmission of the payload data to the total elapsed time [36]. For the proposed

scheme, the saturation throughput is given by:

$$S = (1 - P_{cw}) \frac{(zN_2) E \{ \text{payload} \}}{(N_1 T_1 + T_{grant}) + (zN_2 T_{slot})} \quad (1)$$

where $E \{ \text{payload} \}$ is the average transmit time duration of the payload data within a timeslot in T_{tran} and P_{cw} (the probability of channel waste) is the probability of unsuccessful access during T_{ac} . Assuming that the terminals' request access to the AP has a probability p and T_{tran} is a constant, then we have:

$$P_{cw} = \sum_{m=0}^M p[0|m, N_1] b(M, m, p) \quad (2)$$

where $p[k|m, n]$ is the probability of k successful (collision free) access while m terminals request access to the AP randomly, which will be chosen from n available T_1 in T_{ac} . Next, we have the recursive expression of $p[k|m, n]$ [36], [37] as follows:

$$p[k|m, n] = b[m, 0, 1/n] p[k|m, n-1] + b[m, 1, 1/n] p[k-1|m-1, n-1] + \sum_{i=2}^m b[m, i, 1/n] p[k-m+i, n-1] \quad (3)$$

The initial condition for $p[k|m, n]$ is described in [36]:

$$p[0|0, n] = 1 \quad p[0|1, n] = 0 \\ p[1|0, n] = 0 \quad p[1|1, n] = 1 \quad \text{For all } (n > 0) \quad (4)$$

$b(M, m, p)$ means the binomial distribution of the number of terminals that request access to the AP in T_{ac} , and M is the total number of terminals requesting access to the AP, which can be expressed as follows:

$$b(M, m, p) = \frac{M!}{m!(M-m)!} p^m (1-p)^{M-m} \quad (5)$$

The analytical throughput can be easily determined by substituting P_{cw} . Note that other parameters such as $T_1, T_{grant}, T_{slot}, E \{ \text{Payload} \}, N_1, N_2$ and z are constants.

B. AVERAGE ACCESS LATENCY

For the latency evaluation of the proposed scheme, the average access delay (AAD) described in [36] is adopted, which describes the average time that a terminal must wait prior to a transmission to measure how fast the channel can be accessed and is given as follows:

$$AAD^{(sec)} = (AAD^{(frame)} - 1)(N_1 T_1 + T_{grant} + zN_2 T_{slot}) + (N_1 T_1 + T_{grant} + \frac{N_2}{2} T_{slot}) \quad (6)$$

where

$$AAD^{(frame)} = \sum_{j=0}^{\infty} j \Pr \{ AD = j \} = Q \sum_{j=0}^{\infty} j (1-Q)^{j-1} = \frac{1}{Q} \quad (7)$$

with

$$Q = \Pr \{ AD = 1 \} = p(1 - P_c) \quad (8)$$

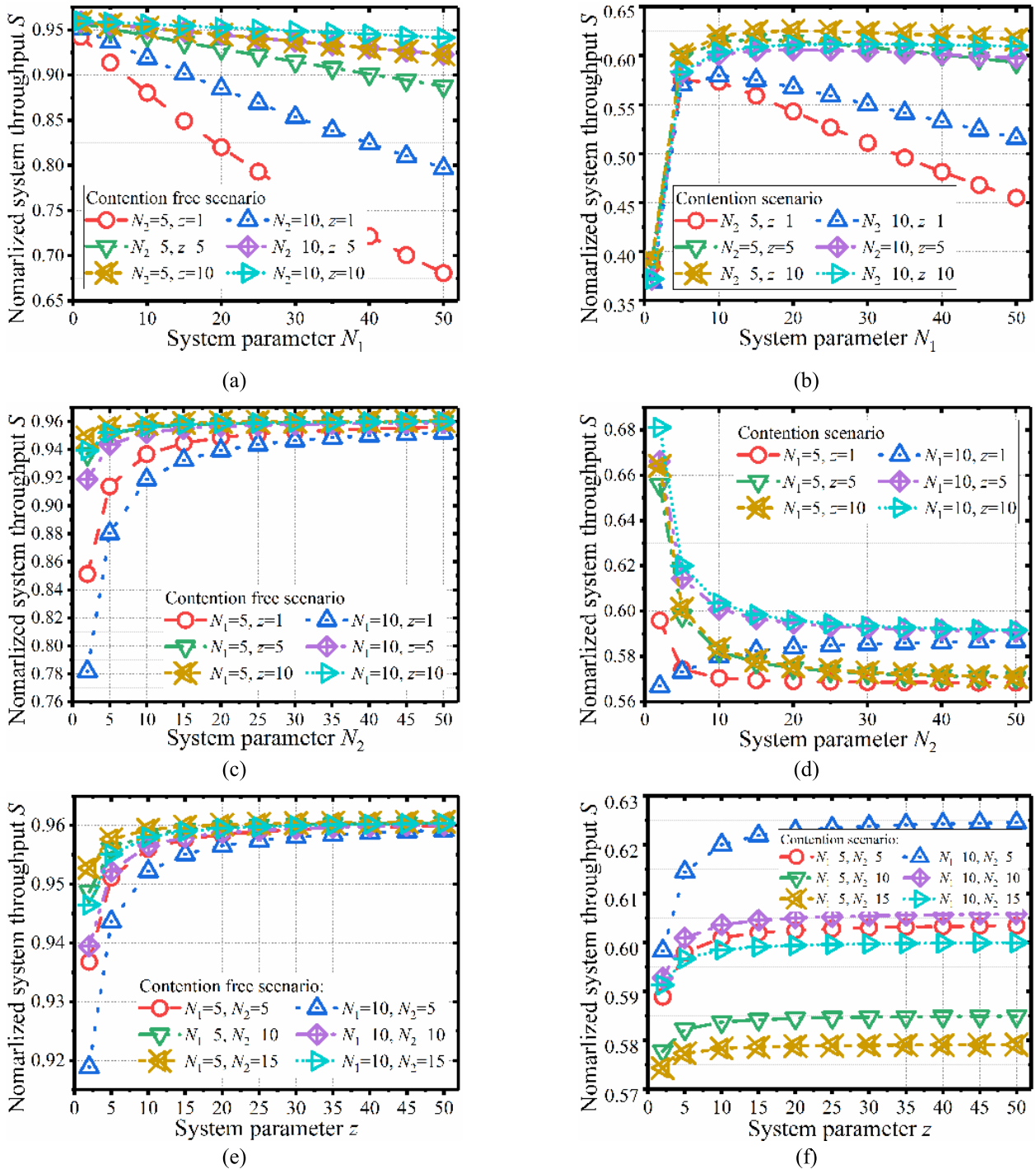


FIGURE 5. System normalized throughput S with a variation in the system special parameters: (a) S with a variation in N_1 in the contention free scenario; (b) S with a variation in N_1 in the contention scenario; (c) S with a variation in N_2 in the contention free scenario; (d) S with a variation in N_2 in the contention scenario; (e) S with a variation in z in the contention free scenario; (f) S with a variation in z in the contention scenario.

and

$$P_c = \sum_{k=0}^{M-1} b(M-1, k, p) \left[1 - \left(\frac{N_1 - 1}{N_1} \right)^k \right] \quad (9)$$

where Q and P_c indicate the probability of access delay (AD) in the current frame and the probability of content,

respectively. Note that $N_1 T_1 + T_{\text{grant}} + z N_2 T_{\text{slot}}$ is equal to the frame time.

From the ADD equation, the terminal will wait for (AAD-1) frames before sending its data in the next frame (i.e., the transmission frame). The terminal will also wait by an additional contention time of $N_1 T_1$ and a grant time of T_{grant} until a timeslot is assigned. The last term $z N_2 T_{\text{slot}}/2$

shows the average waiting time before the main frame is transmitted.

IV. RESULTS AND DISCUSSION

A. SELECTION AND OPTIMIZATION OF THE SYSTEM PARAMETERS

The proposed multiple access scheme introduced three special system parameters, namely, N_1 , N_2 and z , to balance the system throughput and terminal access latency. The selection and optimization of system parameters were discussed in detail for the optimal achievement of the proposed system with a numeral simulation of system metrics mentioned in section III. The numeral simulation was carried out in MATLAB with $E\{\text{Payload}\} = 2048$ Bytes and an R_b of 1 Mbps. The simulation results are demonstrated in Fig. 5.

Fig. 5 (a) and (b) shows the variation in the throughput S as a function of N_1 for a range of N_2 and z with and without contention. Note that in contention free scenarios, S is decreasing linearly with N_1 depending on the values of N_2 and z . The rate of decrease in S is higher for smaller values of N_2 and z . However, in contention scenarios, S exponentially increases with N_1 (up to 5) for all values of N_2 and z and then decreases with N_1 . Therefore, as N_1 increases, the contention becomes less intense, which is desirable.

Fig. 5 (c) and (d) illustrates S as a function of N_2 for a range of N_1 and z with and without contention. In scenarios without and with contentions, S increases and decreases with N_2 reaching maximum and minimum values before saturation. In contention free cases, for a fixed z , S is higher for smaller N_1 , with reduced levels of channel waste in data transmission, which is exactly opposite of the contention scenarios. Notably, in contention scenarios, as shown in Fig. 5 (c) and (d), there is a special curve. For $N_1 = 10$ and $z = 1$, S shows an increasing trend. Here, the calculation of P_{cw} is affected by N_1 , where P_{cw} increases with proper values of N_1 and z . This characteristic in the contention scenario might be a critical factor while defining the system parameters.

Fig. 5 (e) and (f) illustrates S against z for a range of N_1 and N_2 values, which shows almost flat responses with higher values for the contention free cases.

The numerical simulations (in MATLAB) of the AAD^(sec) are outlined in Fig. 6. Fig. 6 (a) shows that the AAD is a function of N_1 and for a range of N_2 and z , where the AAD displays a large value in the contention scenario for $N_1 = 2$. Notably, a large P_c means that the system is competitive with less access resources. For the contention cases, the AAD increases with $N_1 > 3$; i.e., the AAD determined mainly by the access procedure ($N_1 T_1$) in a fixed capacity system. For contention free scenarios, the AAD (sec) decreases with N_1 and remains constant for $N_1 > 4$.

In Fig. 6 (b), the AAD^(sec) increases sharply with N_2 (i.e., an increase in the capacity with N_2), which indicates that the data transmission procedure is longer and the terminals must wait longer times to transmit the data.

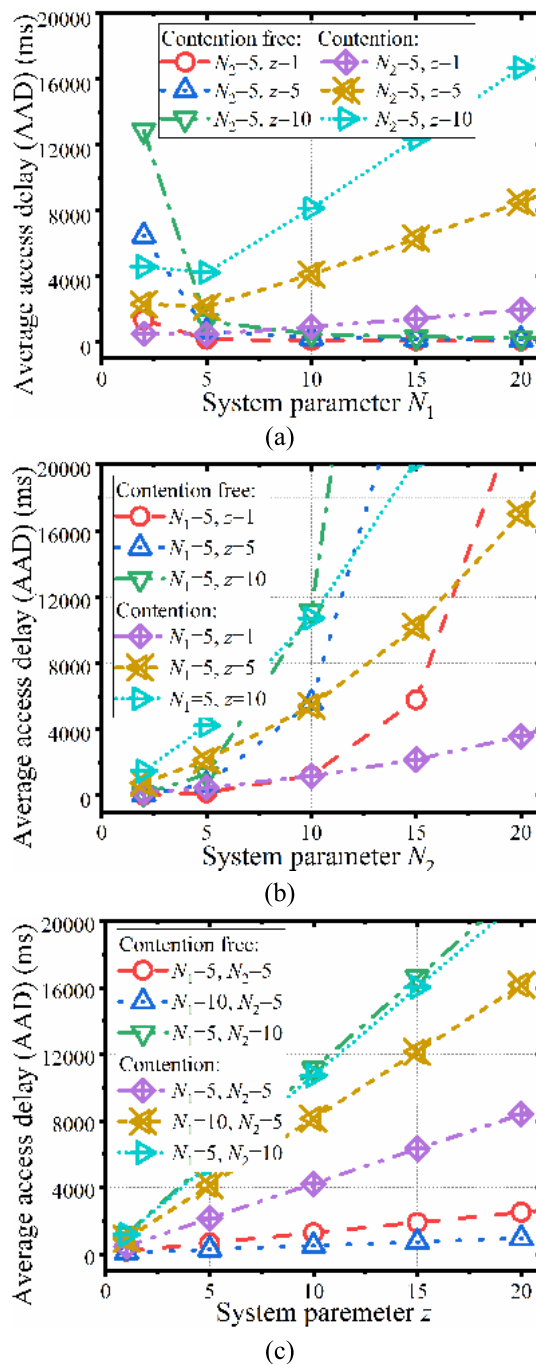


FIGURE 6. Average access delay AAD with a variation in the system special parameters: (a) AAD with a variation in N_1 ; (b) AAD with a variation in N_2 ; (c) AAD with a variation in z .

Fig. 6 (c) illustrates that the AAD^(sec) increases linearly with z and increases more sharply with higher values of N_2 . For fixed N_1 and N_2 , the higher values of z means terminals maintain a longer timeslot assigned in the access procedure. Notably, the throughput and AAD have different trends for different values of N_1 , N_2 and z .

As discussed above, the system metrics of the throughput and access latency vary with the selection of

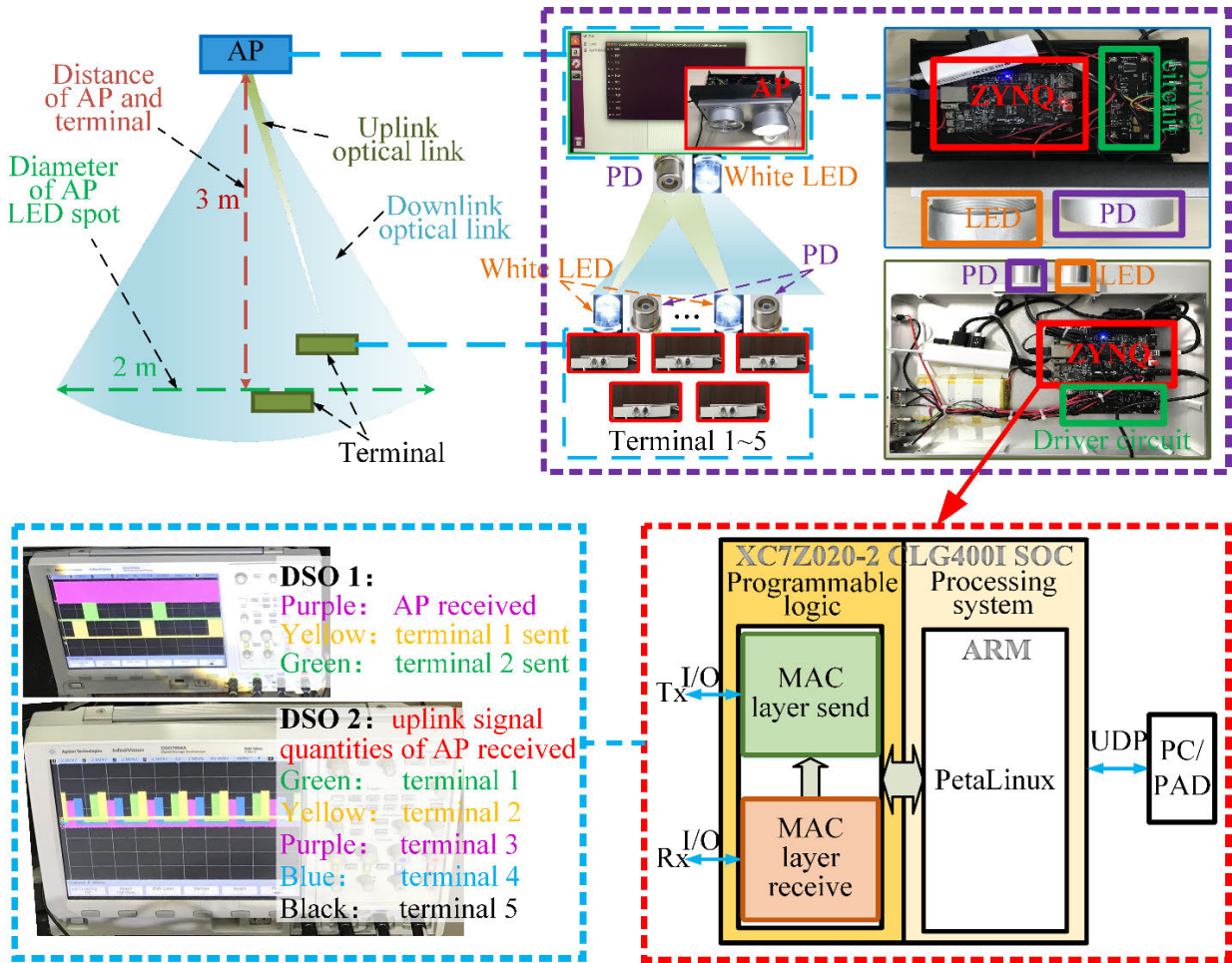


FIGURE 7. Experimental testbed.

system parameters. If different system designs for pure VLC networking using CRMA are required, then the different system parameters of N_1N_2 and z with different R_b values and payload are used. The optimization of the system parameters should be in accordance with purpose of different systems.

B. EXPERIMENTAL SETUP

As shown in Fig. 7, an experimental test bed was developed for the evaluation of the proposed multiple access scheme. The test bed contained one AP and five terminal realizations. The implementation of the proposed CRMA for pure VLC networking system for the AP and five terminals (terminal one to terminal five in Fig. 7) was composed of a development board (from Xilinx (XC7Z020-2 CLG400I SOC)) for running the proposed multiple access scheme, a VLC transmitter (Tx) (i.e., an LED with the driver) and an optical Rx (PD with transimpedance amplifier). In addition, a PC (with an Ubuntu OS installed) connected to the AP served as a server, two PADs (Surface pro with Win10 OS installed) were used as the clients, which were connected to the terminals. As Fig. 7

shows, the distance between the AP and terminals was 3 m. In addition, the projected spot diameter of the AP LED was 2 m.

As illustrated in Fig. 7 with red dashed line, the proposed CRMA scheme was implemented in the programmable logic of XC7Z020-2 SOC. The main function of the proposed scheme is shown in Fig. 2 (c), and the contention avoidance scheme for terminal access to the AP is shown in Fig. 4. Moreover, a PetaLinux operating system was installed on an ARM-based processing system to cooperate with the PC/PADs by using a user datagram protocol (UDP). In PetaLinux, two threads were activated for bidirectional cooperation with the MAC layer send block and MAC layer receive block, respectively.

In the experiments, we evaluated the system metrics of the designed pure VLC networking system with the proposed multiple access scheme with one AP and five terminals in the connectivity between the AP and the terminal and access time of terminal. The parameters in the experimental test bed and numerical systems are listed in the Table 2. In addition,

TABLE 2. Numerical and experimental parameters in the proposed multi-access scheme.

Symbol	Quantity	Comment
R_b	1 Mbps	
N_1	5	
N_2	5	
z	10	
T_l	0.682 ms	
T_{grant}	0.986 ms	
T_{slot}	According to $E\{\text{payload}\}$	$E\{\text{payload}\}/R_b$
p	1	contention free
$E\{\text{payload}\}$	256, 512, 1024 and 2048 Bytes	
Distance between the AP and Terminals	3 m	
Spot diameter of the AP LED	2 m	

an end-to-end traffic was model by using a self-develop program installed on both the PC and PADs to send packets constantly in both the downlink and uplink, respectively. The self-developed program can also receive packets and count the numbers of packets of sent and received packages, respectively, at the same time.

C. EXPERIMENTAL RESULTS AND DISCUSSION

In the experiment, each PC and PAD had a self-developed program to send/receive and count packages which were transmitted between the AP (or PAD) and Zynq-7000 SoC board through a UDP. In addition, each PC and PAD had a Wireshark installed in order to capture the packages, record the number of packages (M) that were transmitted/received and the start/end time of the transmission. For system throughput, the self-developed program sends a file with a large size (e.g., an MP3 with 99.999744 MB in the experiment); as simulated, the network always has packets to transmit. Then, the channel time can be obtained for the successful transmission of the payload data by $T\{\text{payload}\} = ME\{\text{payload}\}$, where M is the number of packages sent. $E\{\text{payload}\}$ is the time transmitted for one payload in $R_b = 1$ Mbps. Then, the system normalized the throughput $S = T\{\text{payload}\}/T_{\text{total}}$, where T_{total} is the total elapsed time of the transmission of each file. However, for the terminal's AAD, we set the size of the file to be equal to that transmitted to the payload, recorded the sent time and received time (note, the system time of the PAD need to be synchronized with PC). Then, through the difference between the received time and sent time, we obtained the duration time for the test terminal to transmit the first package, which was the AAD. The experiment was carried out several times, and we took the average values as the last experimental results shown in Fig. 8. The connectivity of the AP and the five terminals were the signals demonstrated with digital storage oscilloscope (DSO) 1 and DSO 2 in Fig. 7.

Fig. 8 (a) illustrates the analytical, simulated and experimental throughput and the AAD as a function of $E\{\text{payload}\}$.

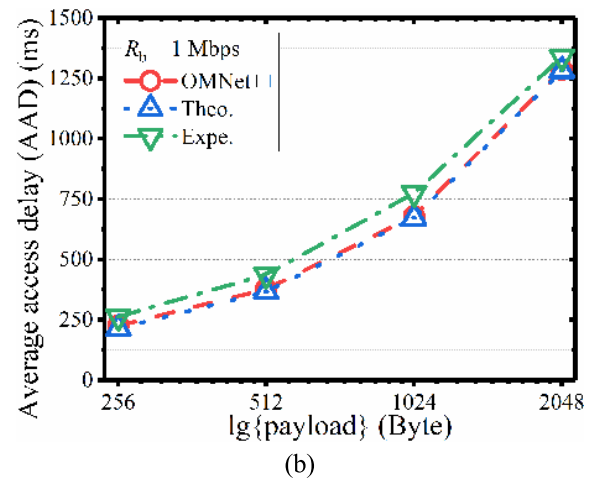
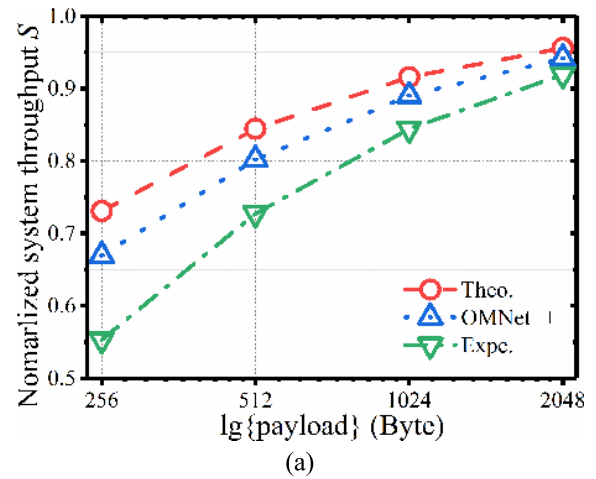


FIGURE 8. Experiment results with a variation in $E\{\text{payload}\}$ compared with theoretical and OMNet++ simulated results: (a) of the system normalized throughput (S); (b) average access delay (AAD).

Note that a relatively low R_b value was adopted to demonstrate the concept with stable connectivity between the AP and the terminals. As shown in Fig. 8 (a), the system's normalized throughput S increases from 0.55, 0.73, and 0.66 to 0.91, 0.95, and 0.94, with $E\{\text{payload}\}$ from 256 Bytes to 2048 Bytes, reaching the saturation levels of 0.91, 0.95 and 0.94 for the experimental, analytical and simulated cases, respectively, at $E\{\text{payload}\} > 2048$ B.

Fig. 8 (b) illustrates the experimental result for the AAD as a function of $E\{\text{payload}\}$ for the contention free scenario for a range of R_b . For R_b of 1 Mbps, the measured, simulated and analytical values for AAD are 263.4, 225.8, and 214.5 ms with payload 256 Bytes, and 1338.6, 1284.8 and 1282.1 ms with payload 2048 Bytes, respectively. Note, we obtain higher values for AAD for $E\{\text{payload}\} > 4096$ Bytes at lower data rates. The results show that a well-designed pure VLC network with a bidirectional VLC link can perform well in a fully networked system. Moreover, in our experiment, five terminals were picked to access one AP one by one dynamically. The results indicate that far more than five terminals could be added by increasing the parameter of N_2 for large-scale deployment.

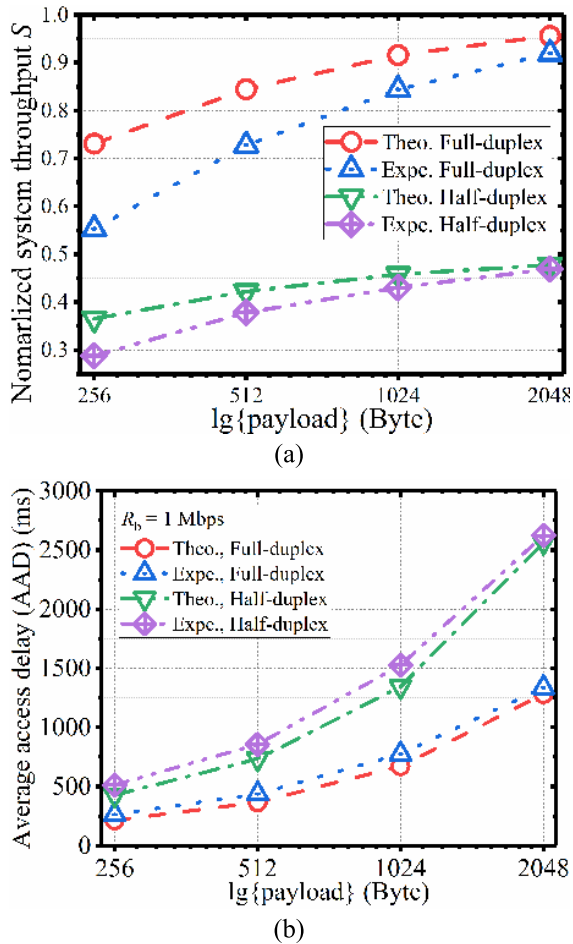


FIGURE 9. Theoretical and experimental results of full-duplex (FD) and half-duplex (HD) with a data rate (R_b) of 1 Mbps: (a) System normalized throughput S ; (b) Average access delay (AAD) of terminal.

D. EXPERIMENTAL COMPARISON OF BIDIRECTIONAL AND HALF-DUPLEX OPERATION

A comparison of the bidirectional operation and half-duplex operation of the proposed CRMA scheme is shown in Fig. 9. In practical cases, as Fig. 9 shows, for the experimental results of the proposed CRMA scheme, the dominance of the system normalized throughput (S) is less than two orders compared with the half-duplex, and the dominance of the AAD is more than a half order compared with the half-duplex. This finding is because of the interference of bidirectional operation.

V. EXTENDED DISCUSSION

The theoretical and experimental results above have proven that the proposed multiple access scheme is feasible for bidirectional VLC networking. In addition, the proposed multiple access scheme is demonstrated to be suitable for higher R_b scenarios. The OMNet++ simulated results of higher R_b values of 5 Mbps, 50 Mbps and 100 Mbps were demonstrated in Fig. 10 with the proposed multiple access scheme with the system parameters listed in Table 2. For $R_b > 50$ Mbps, the AAD is acceptable, which decreases by several ms at an R_b of 100 Mbps. The results show that a well-designed

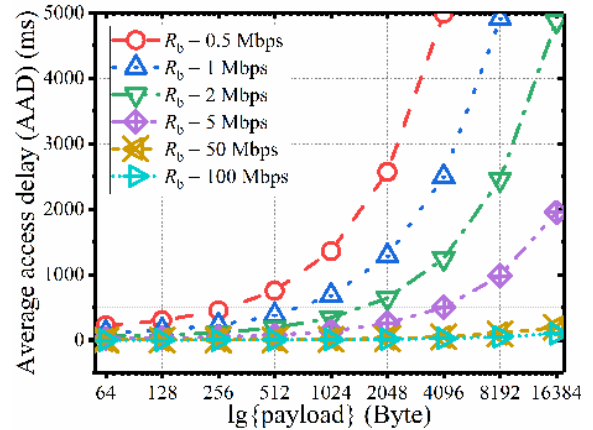


FIGURE 10. OMNet++ simulated results of the average access delay with higher R_b values with a variation in $E\{payload\}$.

pure VLC network with a bidirectional VLC link can perform well in a fully networked system. Notably, with gigabit VLC systems (common rate at present), the proposed multiple access scheme performs well, and the pure VLC network performs better than the state-of-the-art Femtocell networks and the hybrid RF-VLC system in indoor environments as part of 5G networks.

VI. CONCLUSION

A TDD-based centralized-coordinated resources-reserved multiple access scheme to support a bidirectional VLC access network, which does not use infrared (IR) or WiFi for the uplink, was proposed and demonstrated experimentally. The proposed scheme, through the centralized authorization by the AP, is adaptively simplified by the cost of one more handshake between the AP and terminals during the access procedure to reduce the complexity of the data transmit procedure, i.e., no handshake, no carrier sensing and no random back-off before data transmission and no collision during data transmission. Moreover, by introducing the parameters N_1 , N_2 and z , the proposed scheme is an effective and feasible multiple access for a pure VLC network with an enhanced balance of the system throughput and the access latency metrics. The results showed that the normalized throughput is independent of the data rate and the average access delay is improved greatly with an increase in the data rate. Therefore, the proposed scheme is attractive for VLC systems with much higher data rates of 1 Gbps and 2.5 Gbps. Furthermore, the proposed CRMA scheme, which works in a bidirectional scenario, can be used as a supplement in the ongoing IEEE 802.11 bb Std.

REFERENCES

[1] Cisco Visual Networking Index: Global Mobile Data Traffic Forecast Update, 2017-2022 White Paper, Cisco, San Francisco, CA, USA, Feb. 2019.
 [2] I. A. Alimi, A. M. Abdalla, J. Rodriguez, P. P. Monteiro, A. L. Teixeira, S. Zvánovec, and Z. Ghassemlooy, *Enabling VLC and WiFi Network Technologies and Architectures Toward 5G, Optical and Wireless Convergence for 5G Networks*, A. M. Abdalla, J. Rodriguez, I. Elfergani, and A. Teixeira, Eds. Hoboken, NJ, USA: Wiley, 2019, ch. 5, pp. 101–122.

- [3] Z. Ghassemlooy, *Visible Light Communications: Theory and Applications*. Boca Raton, FL, USA: CRC Press, Jun. 2017.
- [4] L. Feng, R. Q. Hu, J. Wang, P. Xu, and Y. Qian, "Applying VLC in 5G networks: Architectures and key technologies," *IEEE Netw.*, vol. 30, no. 6, pp. 77–83, Nov./Dec. 2016.
- [5] H. Alshaer and H. Haas, "Bidirectional LiFi attocell access point slicing scheme," *IEEE Trans. Netw. Service Manage.*, vol. 15, no. 3, pp. 909–922, Sep. 2018.
- [6] E. M. Almohimmah, M. T. Alresheedi, A. F. Abas, and J. Elmighani, "A simple user grouping and pairing scheme for non-orthogonal multiple access in VLC system," in *Proc. 20th Int. Conf. Transparent Opt. Netw. (ICTON)*, Jul. 2018, pp. 1–4, doi: [10.1109/ICTON.2018.8473907](https://doi.org/10.1109/ICTON.2018.8473907).
- [7] H. Shen, Y. Wu, W. Xu, and C. Zhao, "Optimal power allocation for downlink two-user non-orthogonal multiple access in visible light communication," *J. Commun. Inf. Netw.*, vol. 2, no. 4, pp. 57–64, Dec. 2017, doi: [10.1007/s41650-017-0037-3](https://doi.org/10.1007/s41650-017-0037-3).
- [8] S. Feng, T. Bai, and L. Hanzo, "Joint power allocation for the multi-user NOMA-downlink in a power-line-fed VLC network," *IEEE Trans. Veh. Technol.*, vol. 68, no. 5, pp. 5185–5190, May 2019, doi: [10.1109/TVT.2019.2906095](https://doi.org/10.1109/TVT.2019.2906095).
- [9] B. Lin, X. Tang, Z. Ghassemlooy, C. Lin, M. Zhang, Z. Zhou, Y. Wu, and H. Li, "A NOMA scheme for visible light communications using a single carrier transmission," in *Proc. 1st South Amer. Colloq. Visible Light Commun. (SACVLC)*, Nov. 2017, pp. 1–4, doi: [10.1109/SACVLC.2017.8267609](https://doi.org/10.1109/SACVLC.2017.8267609).
- [10] H. Marshoud, V. M. Kapinas, G. K. Karagiannidis, and S. Muhaidat, "Non-orthogonal multiple access for visible light communications," *IEEE Photon. Technol. Lett.*, vol. 28, no. 1, pp. 51–54, Jan. 1, 2016, doi: [10.1109/LPT.2015.2479600](https://doi.org/10.1109/LPT.2015.2479600).
- [11] Z. Tahira, H. M. Asif, A. A. Khan, S. Baig, S. Mumtaz, and S. Al-Rubaye, "Optimization of non-orthogonal multiple access based visible light communication systems," *IEEE Commun. Lett.*, vol. 23, no. 8, pp. 1365–1368, Aug. 2019, doi: [10.1109/LCOMM.2018.2889986](https://doi.org/10.1109/LCOMM.2018.2889986).
- [12] J. Lian and M. Brandt-Pearce, "Multiuser visible light communication systems using OFDMA," *J. Lightw. Technol.*, vol. 38, no. 21, pp. 6015–6023, Nov. 1, 2020, doi: [10.1109/JLT.2020.3008290](https://doi.org/10.1109/JLT.2020.3008290).
- [13] S. Baig, H. Muhammad Asif, T. Umer, S. Mumtaz, M. Shafiq, and J.-G. Choi, "High data rate discrete wavelet transform-based PLC-VLC design for 5G communication systems," *IEEE Access*, vol. 6, pp. 52490–52499, 2018, doi: [10.1109/ACCESS.2018.2870138](https://doi.org/10.1109/ACCESS.2018.2870138).
- [14] M. S. A. Mossaad, S. Hranilovic, and L. Lampe, "Visible light communications using OFDM and multiple LEDs," *IEEE Trans. Commun.*, vol. 63, no. 11, pp. 4304–4313, Nov. 2015, doi: [10.1109/TCOMM.2015.2469285](https://doi.org/10.1109/TCOMM.2015.2469285).
- [15] A. Kuriharat, C.-J. Ahn, T. Otori, and K.-Y. Hashimoto, "An application of OFDM-IDMA to uplink multiuser visible light communication system," in *Proc. Int. Symp. Intell. Signal Process. Commun. Syst. (ISPACS)*, Nov. 2015, pp. 412–416, doi: [10.1109/ISPACS.2015.7432806](https://doi.org/10.1109/ISPACS.2015.7432806).
- [16] M. H. Shoreh, A. Fallahpour, and J. A. Salehi, "Design concepts and performance analysis of multicarrier CDMA for indoor visible light communications," *IEEE/OSA J. Opt. Commun. Netw.*, vol. 7, no. 6, pp. 554–562, Jun. 2015, doi: [10.1364/JOCN.7.000554](https://doi.org/10.1364/JOCN.7.000554).
- [17] S.-H. Chen and C.-W. Chow, "Color-shift keying and code-division multiple-access transmission for RGB-LED visible light communications using mobile phone camera," *IEEE Photon. J.*, vol. 6, no. 6, pp. 1–6, Dec. 2014, doi: [10.1109/JPHOT.2014.2374612](https://doi.org/10.1109/JPHOT.2014.2374612).
- [18] Z. Zheng, T. Chen, L. Liu, and W. Hu, "Experimental demonstration of femtocell visible light communication system employing code division multiple access," in *Proc. Opt. Fiber Commun. Conf.*, Mar. 2015, pp. 1–3, doi: [10.1364/OFC.2015.Tu2G.4](https://doi.org/10.1364/OFC.2015.Tu2G.4).
- [19] A. Khreishah, S. Shao, A. Gharaibeh, M. Ayyash, H. Elgala, and N. Ansari, "A hybrid RF-VLC system for energy efficient wireless access," *IEEE Trans. Green Commun. Netw.*, vol. 2, no. 4, pp. 932–944, Dec. 2018, doi: [10.1109/TGCN.2018.2849944](https://doi.org/10.1109/TGCN.2018.2849944).
- [20] V. K. Papanikolaou, P. D. Diamantoulakis, Z. Ding, S. Muhaidat, and G. K. Karagiannidis, "Hybrid VLC/RF networks with non-orthogonal multiple access," in *Proc. IEEE Global Commun. Conf. (GLOBECOM)*, Dec. 2018, pp. 1–6, doi: [10/ggfttf](https://doi.org/10/ggfttf).
- [21] M. Amjad, H. K. Qureshi, S. A. Hassan, A. Ahmad, and S. Jangsher, "Optimization of MAC frame slots and power in hybrid VLC/RF networks," *IEEE Access*, vol. 8, pp. 21653–21664, 2020, doi: [10.1109/ACCESS.2020.2968624](https://doi.org/10.1109/ACCESS.2020.2968624).
- [22] J. Lian, M. Noshad, and M. Brandt-Pearce, "M-PAM joint optimal waveform design for multiuser VLC systems over ISI channels," *J. Lightw. Technol.*, vol. 36, no. 16, pp. 3472–3480, Aug. 15, 2018, doi: [10.1109/JLT.2018.2846187](https://doi.org/10.1109/JLT.2018.2846187).
- [23] *Status of IEEE 802.11 Light Communication*. Accessed: Jun. 26, 2020. [Online]. Available: http://www.ieee802.org/11/Reports/tgbb_update.htm
- [24] Y. F. Liu, C. H. Yeh, C. W. Chow, Y. Liu, Y. L. Liu, and H. K. Tsang, "Demonstration of bi-directional LED visible light communication using TDD traffic with mitigation of reflection interference," *Opt. Exp.*, vol. 20, no. 21, pp. 23019–23024, Oct. 2012, doi: [10.1364/OE.20.023019](https://doi.org/10.1364/OE.20.023019).
- [25] H. Han, M. Zhang, P. Luo, W. Xu, D. Han, and M. Wu, "Real-time bi-directional visible light communication system," in *Proc. 15th Int. Conf. Opt. Commun. Netw. (ICOON)*, Sep. 2016, pp. 1–3, doi: [10.1109/ICOON.2016.7875721](https://doi.org/10.1109/ICOON.2016.7875721).
- [26] H. Abumarshoud and H. Haas, "Index time division multiple access (I-TDMA) for LiFi systems," in *Proc. IEEE 89th Veh. Technol. Conf. (VTC-Spring)*, Apr. 2019, pp. 1–5, doi: [10.1109/VTCSpring.2019.8746663](https://doi.org/10.1109/VTCSpring.2019.8746663).
- [27] T.-C. Bui and M. Biagi, "TDMA-like infrared uplink with multi-faces photodiode access points," in *Proc. IEEE Int. Conf. Commun. Workshops (ICC Workshops)*, May 2019, pp. 1–5, doi: [10.1109/ICCW.2019.8757166](https://doi.org/10.1109/ICCW.2019.8757166).
- [28] B. M. Masini, A. Bazzi, and A. Zanella, "Vehicular visible light networks with full duplex communications," in *Proc. 5th IEEE Int. Conf. Models Technol. for Intell. Transp. Syst. (MT-ITS)*, Jun. 2017, pp. 98–103, doi: [10.1109/MTITS.2017.8005646](https://doi.org/10.1109/MTITS.2017.8005646).
- [29] P. Lin and L. Zhang, "Full-duplex RTS/CTS aided CSMA/CA mechanism for visible light communication network with hidden nodes under saturated traffic," in *Proc. IEEE Int. Conf. Commun. (ICC)*, May 2018, pp. 1–6, doi: [10.1109/ICC.2018.8422623](https://doi.org/10.1109/ICC.2018.8422623).
- [30] S. Kim. (May 2019). *LC MAC submission*. [Online]. Available: <https://mentor.ieee.org/802.11/dcn/19/11-19-0757-02-00bb-lc-mac-submission.pptx>
- [31] Z. Zhang, Y. Xiao, Z. Ma, M. Xiao, Z. Ding, X. Lei, G. K. Karagiannidis, and P. Fan, "6G wireless networks: Vision, requirements, architecture, and key technologies," *IEEE Veh. Technol. Mag.*, vol. 14, no. 3, pp. 28–41, Sep. 2019, doi: [10.1109/MVT.2019.2921208](https://doi.org/10.1109/MVT.2019.2921208).
- [32] J. Grubor, S. Randel, K.-D. Langer, and J. W. Walewski, "Broadband information broadcasting using LED-based interior lighting," *J. Lightw. Technol.*, vol. 26, no. 24, pp. 3883–3892, Dec. 2008.
- [33] F. Miramirkhani and M. Uysal, "Channel modelling for indoor visible light communications," *Phil. Trans. Roy. Soc. A, Math., Phys. Eng. Sci.*, vol. 378, no. 2169, Apr. 2020, Art. no. 20190187, doi: [10.1098/rsta.2019.0187](https://doi.org/10.1098/rsta.2019.0187).
- [34] N. Serafimovski and C. Han. (May 2019). *TGbb: Evaluation Methodology for MAC Proposals*. [Online]. Available: <https://mentor.ieee.org/802.11/dcn/19/11-19-0848-02-00bb-proposed-evaluation-methodology-for-mac-proposals-docx.docx>
- [35] V. Jungnickel. (May 2019). *MAC Simulation Methodology: Insights from LC Channel Measurements*. [Online]. Available: <https://mentor.ieee.org/802.11/dcn/19/11-19-0916-01-00bb-mac-simulation-methodology-insights-from-lc-channel-measurements.pptx>
- [36] S. Asadollahi, H. H. Refai, and P. G. LoPresti, "Performance comparison of CSMA/CA advanced infrared (AIr) and a new point-to-multipoint optical MAC protocol," in *Proc. 8th Int. Wireless Commun. Mobile Comput. Conf. (IWCMC)*, Aug. 2012, pp. 1149–1153.
- [37] T.-K. Liu, J. A. Silvester, and A. Polydoros, "Performance evaluation of R-ALOHA in distributed packet radio networks with hard real-time communications," in *Proc. IEEE 45th Veh. Technol. Conf. Countdown Wireless 21st Century*, Jul. 1995, pp. 554–558.



QIGUAN CHEN received the B.S. and M.S. degrees from the Beijing University of Posts and Telecommunications (BUPT), Beijing, China, in 2008, and 2011, respectively, where he is currently pursuing the Ph.D. degree with the State Key Laboratory of Information Photonics and Optical Communications (IPOC). From 2011 to 2018, he worked on access network field in Guangzhou, China, from 2011 to 2018, with rich experience in access network theory and engineering. His main research interests include wireless optical networking theory and its application.



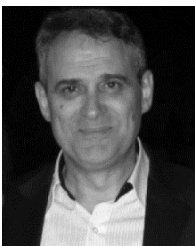
DAHAI HAN received the B.S. degree from Jilin University, China, in 2002, and the Ph.D. degree from BUPT, China, in 2007. He is currently an Associate Professor with the Optical Wireless Communications Group, State Key Laboratory of IPOC, BUPT. His major research interests include UV Communication and detecting and visible light communication.



MIN ZHANG received the Ph.D. degree in optical communications from BUPT, China, where he is currently a Professor, the Deputy Director of the State Key Laboratory of IPOC, and the Deputy Dean of the School of Optoelectronic Information. He holds 45 China patents. He has authored or coauthored more than 300 technical papers in international journals and conferences, and 12 books in the areas of optical communications. His current research interests include optical communication systems and networks, optical signal processing, and optical wireless communications.



ZABIH GHASSEMLOOY (Senior Member, IEEE) joined the University of Northumbria, Newcastle upon Tyne, as the Associate Dean (AD), in 2004. He is currently a Professor. His research interests include optical wireless communications, free space optics, visible light communications, radio over fibre-free space optics, and sensor networks with project funding from EU, U.K. Research Council and industry. He is a C.Eng., Fellow of IET, and Fellow of OSA.



ANTHONY C. BOUCOUVALAS (Fellow, IEEE) received the B.Sc. degree in electrical and electronic engineering from Newcastle upon Tyne University, U.K., in 1978, and the M.Sc. and D.I.C. degrees in communications engineering from the Imperial College, University of London, U.K., in 1979, and the Ph.D. degree in fiber optics from the Imperial College, in 1982. He is currently a Professor. He has published more than 350 articles. He is a Fellow of FIET and FRSA.



ZHIGUO ZHANG received the Ph.D. degree in electronics science and technology from BUPT, China, in 2007. He is currently a Professor with the State Key Laboratory of IPOC, BUPT. His main research interests include advanced optical communication systems and networks, convergent broadband multiservice-access communication systems, optical signal processing, and fiber sensor technologies. He holds 60 China patents. He has authored or coauthored more than 130 technical papers in international journals and conferences.



TONGYAO LI is currently pursuing the degree with the Optical Wireless Communications Group, BUPT, Beijing, China. Her major contribution on experiment.



XIAOTIAN JIANG is currently pursuing the Ph.D. degree with BUPT, Beijing, China. His major contribution on simulation.

...